Electronic Supplementary Material (ESI) for Journal of Materials Chemistry

Scalable Nanomanufacturing of Millimeter-Length 2D Na_xCoO_2 Nanosheets

MahmutAksit, David P. Toledo, and Richard D. Robinson

Department of Materials Science & Engineering, Cornell University, Ithaca, NY, 14853

Electronic Supplementary Information

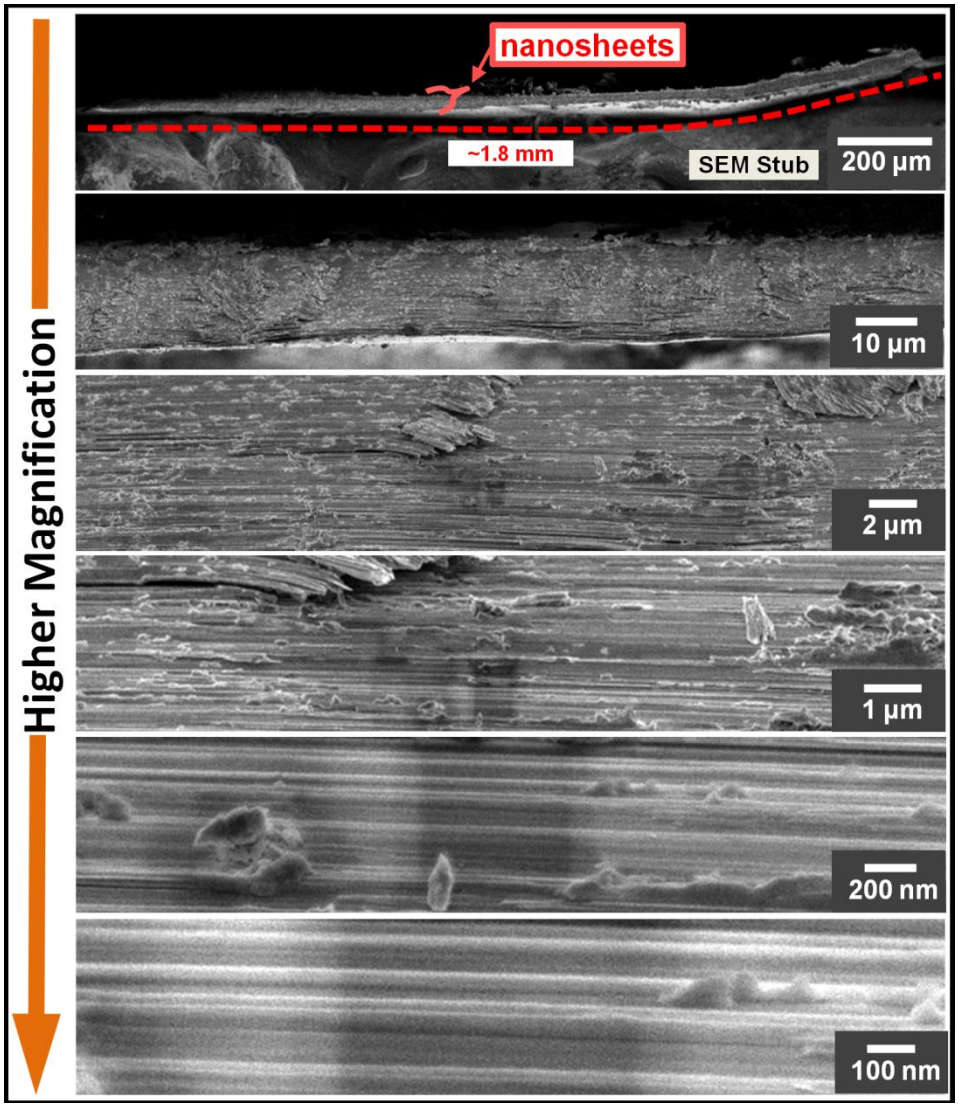

Fig. S1 Additional SEM images for nanosheet metal-oxides. All images show the cross-sections of the stacked nanosheet. Images are sorted from lower magnification to higher magnification.

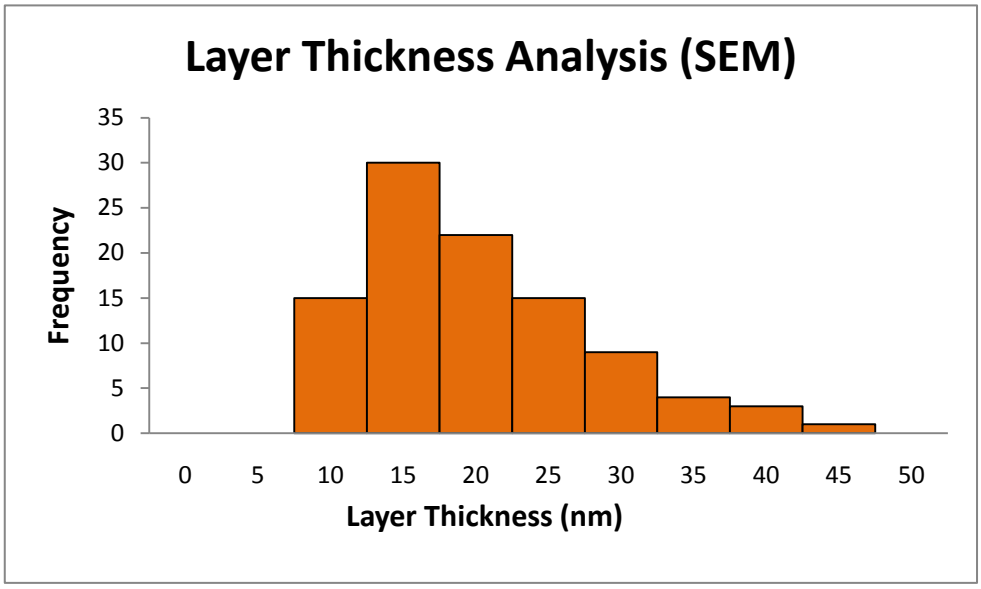

Fig. S2 Histogram of thickness of 100 layers as measured by SEM. The average thickness was found to be 18.2 nm with a median thickness of 16 nm and standard deviation of 7.9 nm.

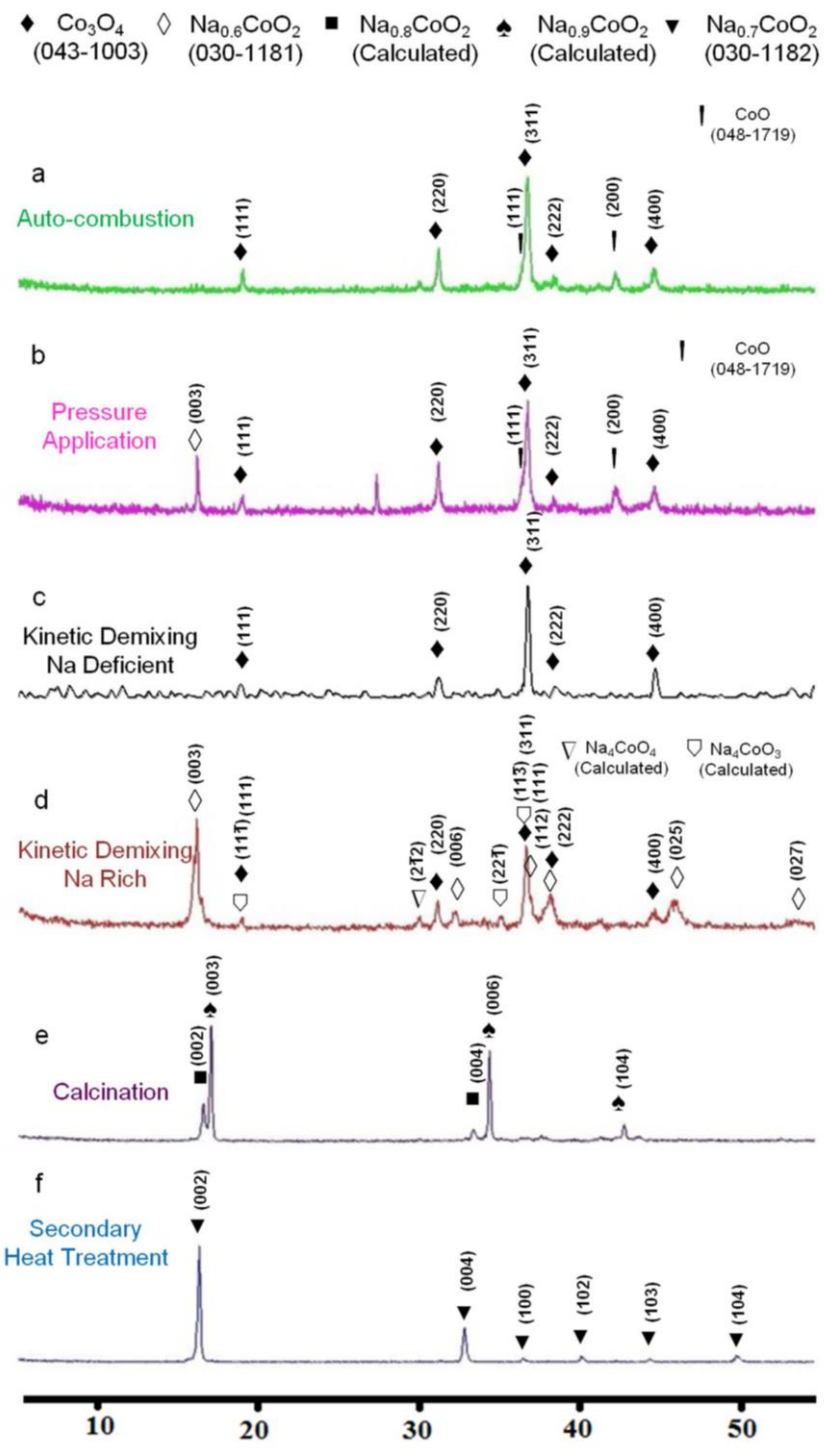

Fig. S3 X-ray powder diffraction of the Na_xCoO_2 between each step of the synthesis procedure. The samples in the form of pellets and singles crystals were ground before the measurement. The peaks are identified for different phases and the available PDF numbers are listed for the phases.

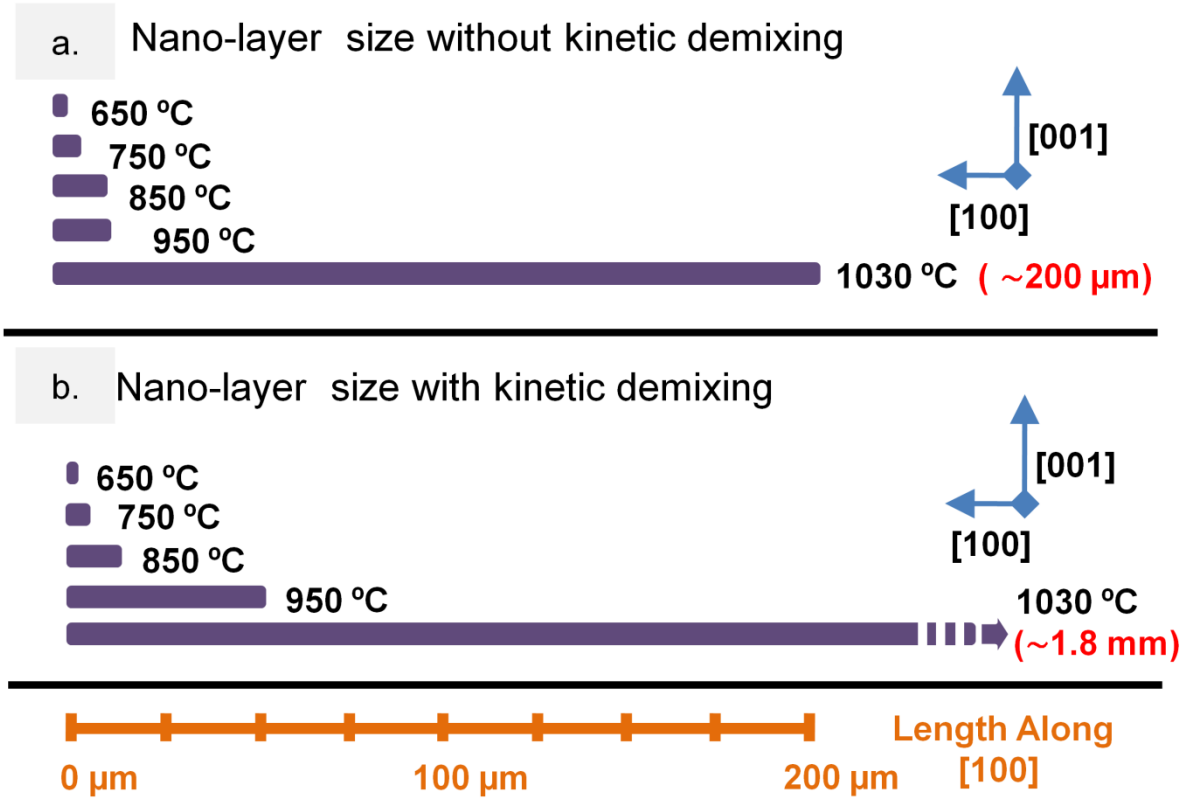

Fig. S4 Schematic diagram representing anisotropic growth of nano-layers at different calcination temperatures without kinetic demixing (a) and with kinetic demixing (b). All samples were initially heated up to 650 ºC and held for 4 hours. The temperature was then rapidly increased up to different values indicated in the figure and calcined for 3 hours. Under both conditions with and without the kinetic demixing significant growth along c axis [001] is not observed. The layers are all at the same thickness around 20 nm. The layers are much longer with kinetically demixed samples. (The bar at the bottom of the figure is to scale with the sizes above)

Cornell High Energy Synchrotron Source (CHESS) G2 Hutch Background

A 0.1% bandwidth slice of the intense beam from the CHESS G-line 50-pole wiggler and multilayer monochromator is deflected into the G2 station by a Be single-crystal beam splitter. The incident beam is collimated vertically by certain number of slits as 1 mm, while the full horizontal beam width of about 2 mm is accepted. The horizontal diffractometer has a motorized sample height stage to precisely align the sample surface into the beam. The scattered beam is detected by a linear gas detector after passing a Soller collimator. Collimator and detector have matching apertures of 8 mm horizontal by100 mm vertical.

For the measurements performed in CHESS G2 Hutch, samples smaller than the beam size are used to increase the penetration depth. Due to the small size of the sample and also the high level of surface roughness, it is expected that the incident beam enters into the material with angles close to 90º at the edges (parallel to (001) planes). It is also known that the beam leaves the material at ~7.5º in order to satisfy the diffraction condition for $(10\bar{1}1)$ plane of $Na_{0.7}CoO_2$. The attenuation length was calculated to be ~2.5 μm at7.5º for the utilized beam energy (8.65 kV) which is equal to the penetration depth relevant to the number of sampled layers.

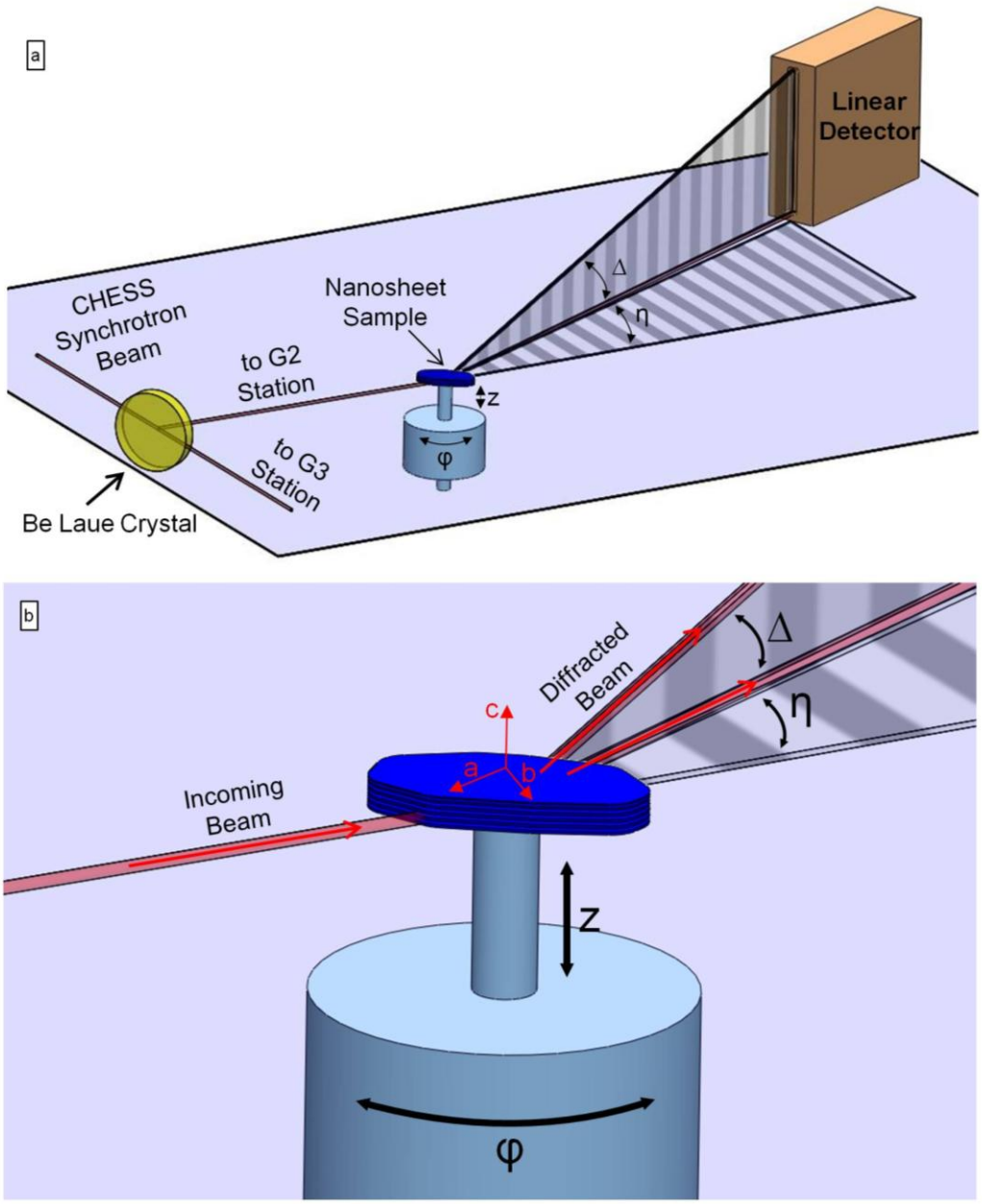

Fig. S5 (a) Schematic representation of the Grazing Incidence Diffraction setup in G line at CHESS. The incident beam comes in at nearly 0º and the diffracted beam is detected by a linear detector which covers 10º along Δ direction. η is set to the 2θ position on the horizontal crystallographic plane. The sample rotates around the φ axis during the scan. (b) A closer look at the sample-beam orientation indicating nanosheets lying parallel to the incident beam.

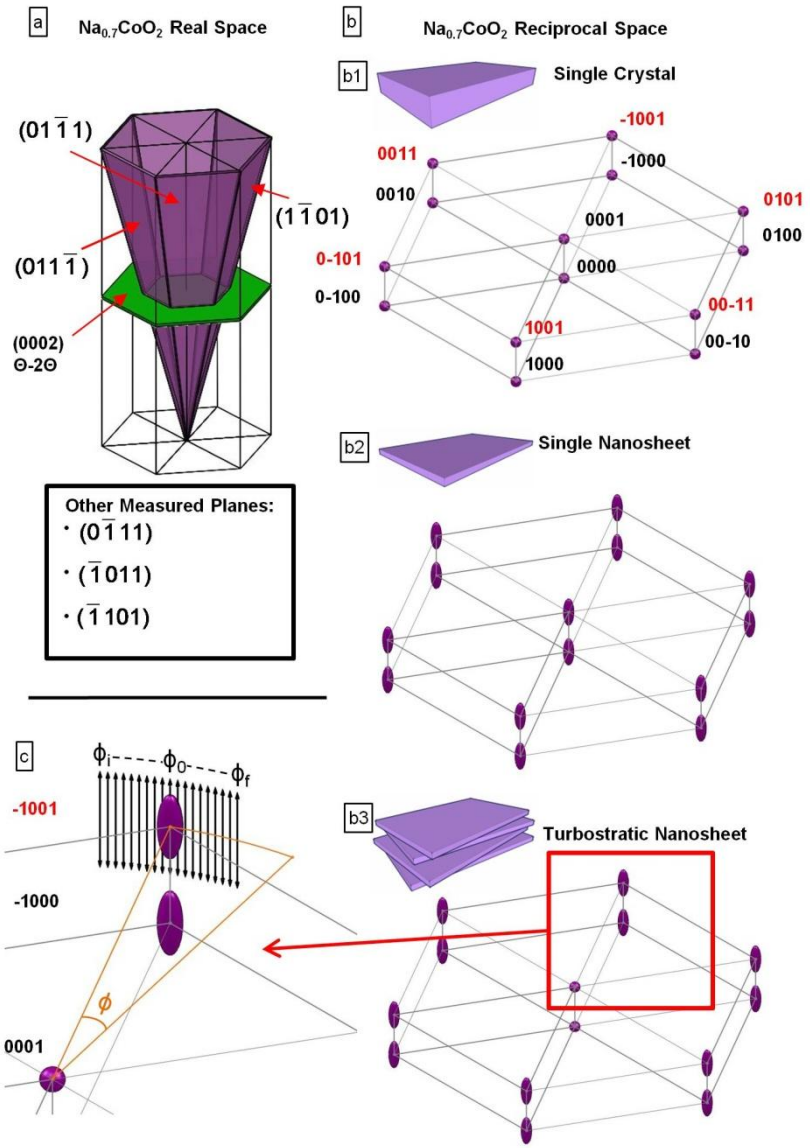

Fig. S6 Schematic of the real (a) and reciprocal (b) space representation of the Na_xCoO_2 lattice. The red arrows in (a) point to $(011\bar{1})$, $(01\bar{1}1)$ and $(1\bar{1}01)$. Shown in part b is the expected reciprocal lattice for a single crystal (b1), single nanosheets (b2), and stack turbostratic nanosheets (b3). The spots observed in a single crystal are broadened due to the finite size effects of the nanosheets. Part c is a schematic of a grazing scan in progress, with $\varphi_i - \varphi_f$ representing the rods seen in Fig 3c of the main text. The rotation of the sample in the ϕ axis causes rotation of the linear detector relative to the reciprocal space. As a result, a θ-2θ type of scan is obtained along the linear detector (along Δ, which corresponds to [001]) for each ϕ value as shown in the figure. Therefore each column of pixels of ϕ in Figure 3c is analogous to a scan represented by arrows in the figure above. Thus the resulting broadening corresponds to finite size along [001].

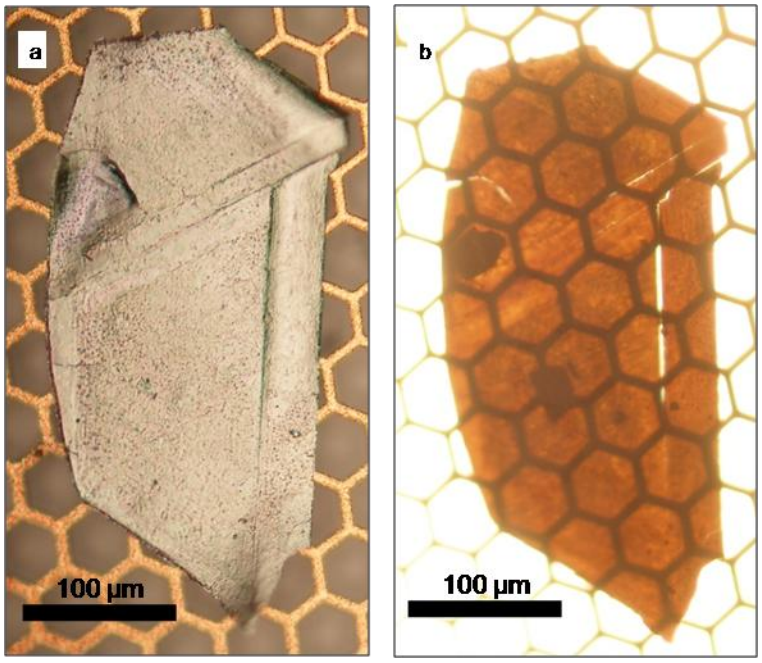

Fig. S7 Optical microscope image taken in reflected (a) and transmitted (b) white light of a large exfoliated nanosheets. The features on the images bellow correlate well with those observed in TEM (Figure 4a main text).

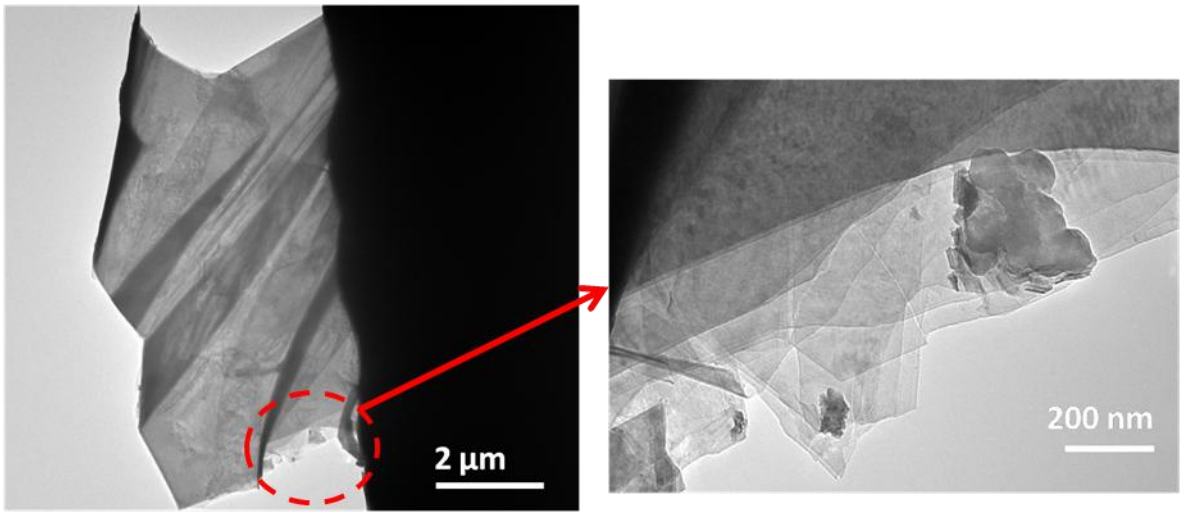

Fig. S8 TEM images showing single layers on the edge of an exfoliated nanosheets. This provides a useful method of measuring the thickness of the exfoliated piece.